

Single-Molecule Resolution of an Organometallic Intermediate in a Surface-Supported Ullmann Coupling Reaction

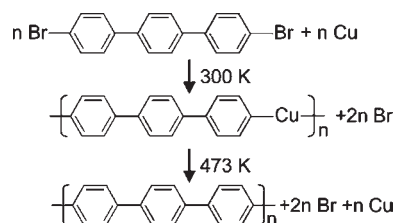
Weihua Wang,[†] Xingqiang Shi,[‡] Shiyong Wang,[†] Michel A. Van Hove,[‡] and Nian Lin^{*,†}

[†]Department of Physics, The Hong Kong University of Science and Technology, Hong Kong, China

[‡]Department of Physics and Materials Science, City University of Hong Kong, Hong Kong, China

ABSTRACT: We have studied the organometallic intermediate of a surface-supported Ullmann coupling reaction from 4, 4'-dibromo-*p*-terphenyl to poly(*para*-phenylene) by scanning tunneling microscopy/spectroscopy and density functional theory calculations. Our study reveals at a single-molecular level that the intermediate consists of biradical terphenyl (ph)₃ units that are connected by single Cu atoms through C–Cu–C bridges. Upon further increasing the temperature, the neighboring biradical (ph)₃ units are coupled by C–C bonds forming poly(*para*-phenylene) oligomers while the Cu atoms are released.

Scheme 1. Surface-Supported Ullmann Coupling Reaction of Br-(ph)₃-Br to Poly(*para*-phenylene) via the Organometallic Intermediate



The Ullmann reaction, a coupling reaction between halogen aromatics via copper catalysts,¹ has long been employed to link aromatic units through C–C bonds in organic synthesis.² Recently this protocol has been introduced to surface, i.e., invoking C–C coupling reactions on a reactive surface. This approach has been exploited to build one-dimensional (1D) molecular wires,^{3–5} nanoribbons,⁶ or two-dimensional (2D) covalent organic networks^{7–11} through depositing halogen aromatics on a surface in ultrahigh vacuum conditions. In addition to the novel structures formed, the studies of the surface-supported coupling reactions provide unprecedented single-molecule insights of these reactions owing to the high resolution of scanning tunneling microscopy (STM).¹² For example, individual molecules of the initial reactants as well as the final products of the reactions have been imaged by STM.^{4,8,10,13,14} Furthermore, transient stage dehalogenation has been observed, too.^{4,8,9,11,14–16} An intermediate state in which the aromatic monomers are brought together, but not yet reacted to form the C–C coupling, has been proposed by several groups.^{4,8,11,13,16,17} This intermediate plays an important role in Ullmann coupling reactions, and the study of its formation and structure can provide important details of the reaction mechanisms and dynamics.^{14,17} However, the signatures of this intermediate state remain ambiguous and controversial: McCarty and Weiss proposed the radicals in the intermediate were connected by molecule–molecule and surface-mediated interactions;^{13,18} Rosei et al. and Lackinger et al. postulated another mechanism of a Cu atom linked intermediate based on the short distance between two neighboring radicals.^{4,8,16}

In this communication, using STM measurements combined with density-functional theory (DFT) calculations, we provide unambiguous evidence at a single-molecule resolution for an organometallic intermediate consisting of C–Cu–C bridges. As shown in Scheme 1, at 300 K monomers of 4,4'-dibromo-*p*-

terphenyl (Br-(ph)₃-Br) undergo debromination reactions on a Cu(111) surface, and the resultant (ph)₃ biradicals are linked by single Cu atoms forming a polymeric organometallic intermediate; at 473 K the C–C coupling takes place, and the intermediate is converted into poly(*para*-phenylene) oligomers, while the Cu atoms are released.

Figure 1a is a large-scale STM image showing at 77 K the Cu(111) surface is covered by a 2D network with a honeycomb structure after depositing the molecules on the surface. The molecules in the network lie along the [11 $\bar{2}$] or equivalent directions of the Cu(111) surface. The periodicity of the network (which is the distance between two neighboring cavities) is 31.5 ± 1.0 Å. The sample was prepared at 77 K on which the density of surface Cu adatom gas was significantly reduced (the density depends on the temperature exponentially);¹⁹ therefore, metal coordination is ruled out as the intermolecular binding in this network. A high-resolution STM image shown in the inset of Figure 1a reveals the ends of three molecules are joined in a vortex manner. The molecular structural model is overlaid in the inset, showing the terminal Br atom (in red) pointing toward a H atom of the neighboring molecule. The distance between the Br and the H is 3.2 ± 0.5 Å, falling in the range of hydrogen bond.²⁰ We propose the honeycomb structure is stabilized by Br···H–C hydrogen bonds. Thus, this structure hints the Br-(ph)₃-Br molecules are intact at 77 K and they are the initial reactants of the coupling reaction.

To study the coupling reaction step by step, we annealed the sample from 77 to 473 K in three steps. After annealing at 473 K (the last step), we observed continuous linear chains on the surface. As shown in Figure 1d, there is no apparent periodicity in the linear chains, except some randomly distributed depressed regions. Electronic band structures of poly(*para*-phenylene) oligomers were observed on these linear chains.²¹ Both topographic

Received: May 30, 2011

Published: July 18, 2011

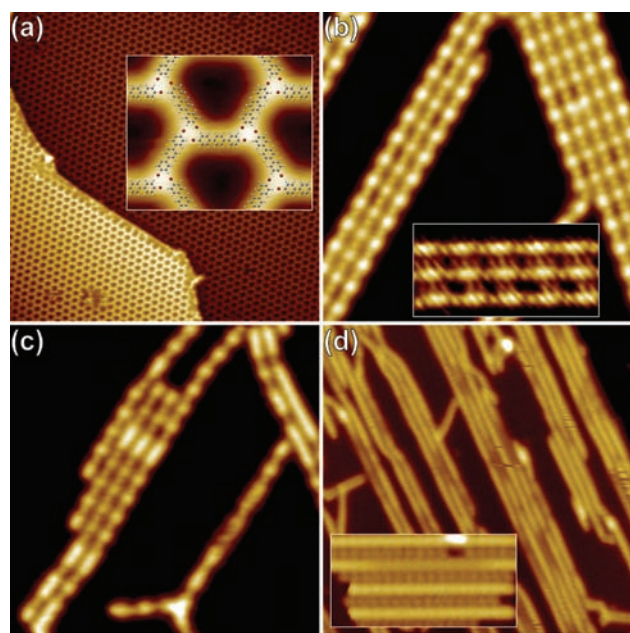


Figure 1. (a) STM image of the as-prepared sample stabilized at 77 K ($120 \times 120 \text{ nm}^2$, 1.0 V, 0.2 nA). (Inset) Magnified STM image of the network ($6 \times 5 \text{ nm}^2$, 1.0 V, 0.2 nA), superimposed with the molecular structural model (Br atoms shown in red). (b) STM image of the sample annealed to 300 K ($20 \times 20 \text{ nm}^2$, 1.0 V, 0.3 nA). (Inset) ($8 \times 4 \text{ nm}^2$, -1.0 V , 0.5 nA) Br atoms lying between the linear periodical structures. (c) STM image of the sample annealed to 393 K ($20 \times 20 \text{ nm}^2$, 1.0 V, 0.2 nA). (d) STM image of the sample annealed to 473 K ($40 \times 40 \text{ nm}^2$, 1.0 V, 0.5 nA). (Inset) ($8 \times 4 \text{ nm}^2$, -1.0 V , 0.5 nA) Br atoms between the poly(*para*-phenylene) oligomers.

and electronic features indicate these linear chains are poly(*para*-phenylene) oligomers, so they are the final product of C–C-coupling reactions. We observed the other product of the reactions, Br atoms, on the surface. They were distributed between the chains as represented by the dotlike features in the inset of Figure 1d (see detail discussion later).

We now discuss the structures formed in the intermediate annealing steps. In the first step, the sample was annealed to 300 K. Figure 1b shows this annealing converted the 2D honeycomb network to extended linear structures. In contrast to the final product (the continuous linear chains after 473 K annealing), here the linear structures exhibit a periodical feature. At a bias voltage of 1.0 V, the STM data reveal the linear structure consists of alternately arranged, brighter, larger oval features and dimmer, smaller round features. These linear periodical structures mainly follow the $[11\bar{2}]$ or equivalent directions of Cu(111) surface. Interestingly, these structures can run across the monatomic steps of the surface, implying that they are robust enough to overcome the perturbation caused by the steps.¹³ Obviously the linear periodical structure is an intermediate state in the reaction from the initial reactant of Br-(ph)₃-Br molecules to the final product of poly(*para*-phenylene) oligomers. Figure 1c shows an STM image of the sample annealed at 393 K. Besides the periodical features observed in Figure 1b, bright segments of different length but without internal periodicity emerge in the linear structures. We will discuss later that these segments are an early stage of the final product, i.e., short poly(*para*-phenylene) oligomers.

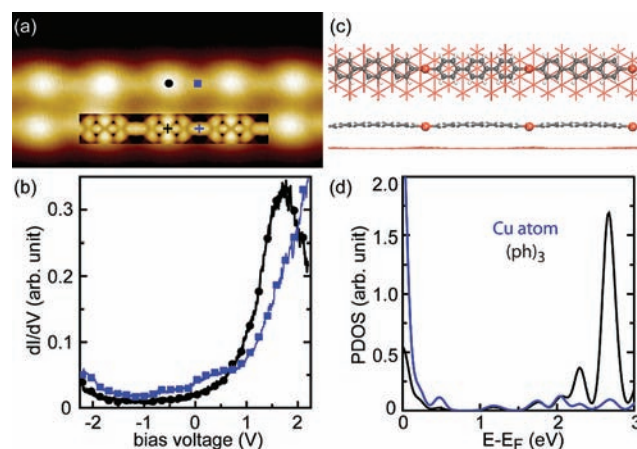


Figure 2. (a) High-resolution STM image of the intermediate ($8 \times 4 \text{ nm}^2$, 1.0 V, 0.5 nA). (Inset) Simulated STM image at +2.7 V on the same scale. (b) dI/dV spectra measured at (ph)₃ (black ●) and Cu atom (blue ■) sites as marked in (a). (c) Top and side views of the optimized structure of the intermediate obtained by the DFT calculation. (d) Calculated PDOS of (ph)₃ unit (black) and Cu atom (blue) as marked by the crosses in (a).

In the inset of Figure 1b, dotlike features can be seen between the linear periodical structures; some dots are arranged in groups of three and the others in groups of two. The random distribution of these dots rules out that they are features contributed by the periodical structures. Similar dotlike features were observed in iodine-aromatic systems adsorbed on a Cu(110) surface and assigned as dissociated iodine atoms adsorbed on the surface.⁴ There were reports that on a Cu(111) surface Br atoms are dissociated from the phenyl group at 300 K.^{8,14,16} We count the number of the dots and estimate that the ratio of these dots and the big oval features in the linear periodical structures is about 2:1. This ratio suggests that the dots represent the Br atoms dissociated from the Br-(ph)₃-Br molecules and adsorbed on the Cu(111) surface subsequently,²² and the brighter oval features represent the resultant (ph)₃ biradicals.

To reveal how the (ph)₃ biradicals units are linked in the intermediate, we examined the structural and the electronic characteristics of the intermediate. The linear periodical structures are commensurate with the Cu lattice in the $[11\bar{2}]$ direction: each three periods matches 11 Cu atoms in this direction, amounting to a periodicity of $16.2 \pm 0.2 \text{ \AA}$. This distance is much larger than the length of a debrominated (ph)₃ biradical, 11.4 Å, as calculated by DFT. We propose that the neighboring (ph)₃ biradicals are connected by Cu atoms (shown as the small features in Figure 2a), and so the linear periodical structures are in fact organometallic intermediates. It is known at the annealing temperature of 300 K, Cu surface provides appreciable amount of Cu atoms as 2D adatom gas, which may be incorporated in the organometallic intermediate.¹⁹ Figure 2c shows a DFT optimized linear periodical structure in which the neighboring (ph)₃ units are linked by a C–Cu–C bridge. The side view shows that, in the optimized structure, the Cu atoms are nearly in the same plane of the phenyl rings and each Cu atom forms two C–Cu bonds with its neighboring (ph)₃ units with a bond length of 2.11 Å. It is worthwhile to note that the Cu atoms do not bind strongly to the Cu substrate, allowing the chain to slide easily on the surface, e.g. across surface steps.

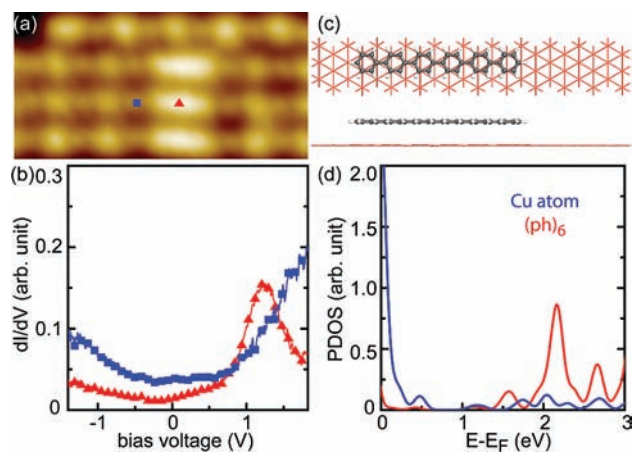


Figure 3. (a) STM image of the intermediate annealed to 393 K ($8 \times 4 \text{ nm}^2$, 1.0 V, 0.2 nA). (b) dI/dV spectra measured at $(\text{ph})_6$ (red \blacktriangle) and Cu atom (blue \blacksquare) sites as marked in (a). (c) Structure of $(\text{ph})_6$ used in the calculation. (d) Calculated PDOS of $(\text{ph})_6$ (red) and Cu atom (blue).

To further understand the properties of the intermediate, we performed tunneling spectra (dI/dV) experiments at different sites in the linear periodical structures. As shown in Figure 2b, in the experimental bias range of -2.2 V to $+2.2 \text{ V}$, the $(\text{ph})_3$'s state shows a prominent peak at $+1.7 \text{ V}$, whereas the Cu atom's state shows a gradual rise starting from $+1.0 \text{ V}$. The calculated projected density of states (PDOS) of the $(\text{ph})_3$ and Cu atom in the intermediate are shown in Figure 2d. The Cu atom has no apparent state, while the $(\text{ph})_3$ shows an electronic state at $+2.7 \text{ V}$. Taking into account that the Fermi level is often offset in the DFT calculations, the calculated PDOS are in fair agreement with the experimental dI/dV spectra. Inset of Figure 2a shows a simulated STM image of the intermediate at $+2.7 \text{ V}$ which reproduces the main features of the experimental STM images.

The shortest segments identified at the 393 K annealed sample have uniform length of 2.5 nm, amounting the length of a $(\text{ph})_6$ oligomer. Figure 3b shows the dI/dV spectra measured at such a segment as well a Cu atom site marked in Figure 3a. The Cu atom exhibits electronic features similar to the one shown in Figure 2b. The $(\text{ph})_6$ oligomer has a peak at $+1.2 \text{ V}$, which is 0.5 V lower than the peak measured on the $(\text{ph})_3$. This is consistent with the reported result of an isolated $(\text{ph})_6$ oligomer.²¹ The calculated PDOS of a $(\text{ph})_6$ oligomer shows an electronic state at $+2.2 \text{ V}$ (cf. Figure 3d), which is 0.5 V lower than the calculated electronic state of $(\text{ph})_3$. The relative energy difference of calculated electronic states of $(\text{ph})_3$ and $(\text{ph})_6$ is in good agreement with the experimental results. Hence, both the topographic and the electronic characteristics of the bright segments strongly suggest they are short poly(*para*-phenylene) oligomers formed by covalent linkage of several $(\text{ph})_3$ units. It is worthwhile to point out that, after the coupling reaction, the length of the poly(*para*-phenylene) oligomers ($(\text{ph})_{3n}$) becomes shorter than the linear periodical structure containing same number (n) of $(\text{ph})_3$ units, presumably due to the fact that Cu atoms in the organometallic intermediate are released in the coupling reactions. All this evidence implies coupling reactions may occur at 393 K at some sites. As the bright segments appear at different locations in the linear periodical structures, the coupling reactions have taken place at different sites. Figure 1d reveals that complete dissociation of the Cu atom occurred when the sample was annealed at 473 K.

In summary, we have studied the organometallic intermediate of the surface-supported Ullmann coupling reaction of $\text{Br}-(\text{ph})_3-\text{Br}$ to poly(*para*-phenylene) by STM measurements and DFT calculations. Our study reveals, at the single-molecule resolution, that the intermediate is an organometallic structure consisting of C–Cu–C bridge-connected biradical $(\text{ph})_3$ units. Upon further increasing the temperature, the neighboring biradical $(\text{ph})_3$ units are linked by C–C bonds forming poly(*para*-phenylene) oligomers while the Cu atoms are released. The Cu atoms act as catalysts in this reaction, and our study confirms the decisive role of transition metal atoms as catalysts in the surface-supported Ullmann coupling reaction.

The experiments were carried out in a commercial ultrahigh vacuum scanning tunneling microscope system (Omicron GmbH) operated at low temperature. The $\text{Br}-(\text{ph})_3-\text{Br}$ molecules were evaporated from a molecular beam evaporator (DODECON nanotechnology GmbH) at approximately 490 K and deposited onto a clean Cu(111) substrate which had been cooled down to 77 K before deposition. After deposition the sample was immediately transferred into the low-temperature STM. To study the coupling reaction step by step, the sample was annealed to temperatures of 300, 393 and 473 K step by step. All the STM measurements were conducted at 77 or 4.9 K. Density-functional theory calculations were performed within the projector-augmented wave (PAW) plane-wave approach as implemented in the VASP code.^{23,24} The exchange-correlation functional was treated with the generalized gradient approximation in the Perdew–Burke–Ernzerhof (PBE) form.²⁵ The surface cell in the calculation is a Cu(111)- $(11\sqrt{3} \times 3)$ rectangle, which contains 66 Cu atoms per surface layer and three $(\text{ph})_3$ -Cu units. Due to the large unit cell (i.e., the computational cost), we adopt only one substrate layer in simulation, which has been proved to give reliable structural and electronic properties for physisorption.^{26,27} The STM images were simulated in constant current mode with the Tersoff–Hamann approximation (i.e., computing an isodensity surface $z(x,y)$ above the adsorbed molecule or surface).²⁸ The planar geometries of the intermediate in Figure 2c and the $(\text{ph})_6$ oligomer in Figure 3c were obtained by structural optimization from an initial geometry of planar phenyl rings. In reality, there may be a nonzero twisting angle between the neighboring phenyl rings. However, the nonzero twisting angle only shifts the PDOS peak of $(\text{ph})_3$ and $(\text{ph})_6$ with respect to the Fermi level²¹ but does not affect the PDOS of Cu atom in the calculations. Therefore, the calculated PDOS of $(\text{ph})_3$, $(\text{ph})_6$, and Cu atom are still in fair agreement with the experimental results.

AUTHOR INFORMATION

Corresponding Author

phnlin@ust.hk.

ACKNOWLEDGMENT

This work is financially supported by Hong Kong RGC under Grant No. 602409, CityU 102408, and the CityU Centre for Applied Computing and Interactive Media.

REFERENCES

- Ullmann, F.; Bielecki, J. *Ber. Deutsch. Chem. Ges.* **1901**, *34*, 2174.
- Hassan, J.; Sévignon, M.; Gozzi, C.; Schulz, E.; Lemaire, M. *Chem. Rev.* **2002**, *102*, 1359.

- (3) Lafferentz, L.; Ample, F.; Yu, H.; Hecht, S.; Joachim, C.; Grill, L. *Science* **2009**, *323*, 1193.
- (4) Lipton-Duffin, J. A.; Ivasenko, O.; Perepichka, D. F.; Rosei, F. *Small* **2009**, *5*, 592.
- (5) Bombis, C.; Ample, F.; Lafferentz, L.; Yu, H.; Hecht, S.; Joachim, C.; Grill, L. *Angew. Chem., Int. Ed.* **2009**, *48*, 9966.
- (6) Cai, J.; Ruffieux, P.; Jaafar, R.; Bieri, M.; Braun, T.; Blankenburg, S.; Muoth, M.; Seitsonen, A. P.; Saleh, M.; Feng, X.; Müllen, K.; Fasel, R. *Nature* **2010**, *466*, 470.
- (7) Grill, L.; Dyer, M.; Lafferentz, L.; Persson, M.; Peters, M. V.; Hecht, S. *Nat. Nanotechnol.* **2007**, *2*, 687.
- (8) Gutzler, R.; Walch, H.; Eder, G.; Kloft, S.; Heckl, W. M.; Lackinger, M. *Chem. Commun.* **2009**, 4456.
- (9) Bieri, M.; Treier, M.; Cai, J.; Ait-Mansour, K.; Ruffieux, P.; Gröning, O.; Gröning, P.; Kastler, M.; Rieger, R.; Feng, X.; Müllen, K.; Fasel, R. *Chem. Commun.* **2009**, 6919.
- (10) Blunt, M. O.; Russell, J. C.; Champness, N. R.; Beton, P. H. *Chem. Commun.* **2010**, 46, 7157.
- (11) Bieri, M.; Nguyen, M.-T.; Gröning, O.; Cai, J.; Treier, M.; Ait-Mansour, K.; Ruffieux, P.; Pignedoli, C. A.; Passerone, D.; Kastler, M.; Müllen, K.; Fasel, R. *J. Am. Chem. Soc.* **2010**, *132*, 16669.
- (12) Hla, S.-W.; Bartels, L.; Meyer, G.; Rieder, K.-H. *Phys. Rev. Lett.* **2000**, *85*, 2777.
- (13) McCarty, G. S.; Weiss, P. S. *J. Am. Chem. Soc.* **2004**, *126*, 16772.
- (14) Blake, M. M.; Nanayakkara, S. U.; Claridge, S. A.; Fernández-Torres, L. C.; Sykes, E. C. H.; Weiss, P. S. *J. Phys. Chem. A* **2009**, *113*, 13167.
- (15) McCarty, G. S.; Weiss, P. S. *J. Phys. Chem. B* **2002**, *106*, 8005.
- (16) Walch, H.; Gutzler, R.; Sirtl, T.; Eder, G.; Lackinger, M. *J. Phys. Chem. C* **2010**, *114*, 12604.
- (17) Nguyen, M.-T.; Pignedoli, C. A.; Passerone, D. *Phys. Chem. Chem. Phys.* **2011**, *13*, 154.
- (18) Sykes, E. C. H.; Han, P.; Kandel, S. A.; Kelly, K. F.; McCarty, G. S.; Weiss, P. S. *Acc. Chem. Res.* **2003**, *36*, 945.
- (19) Lin, N.; Payer, D.; Dmitriev, A.; Strunskus, T.; Wöll, C.; Barth, J. V.; Kern, K. *Angew. Chem., Int. Ed.* **2005**, *44*, 1488.
- (20) Barth, J. V. *Annu. Rev. Phys. Chem.* **2007**, *58*, 375.
- (21) Wang, S.; Wang, W.; Lin, N. *Phys. Rev. Lett.* **2011**, *106*, 206803.
- (22) Nanayakkara, S. U.; Sykes, E. C. H.; Fernández-Torres, L. C.; Blake, M. M.; Weiss, P. S. *Phys. Rev. Lett.* **2007**, *98*, 206108.
- (23) Blöchl, P. E. *Phys. Rev. B* **1994**, *50*, 17953.
- (24) Kresse, G.; Furthmüller, J. *Comput. Mater. Sci.* **1996**, *6*, 15.
- (25) Perdew, J. P.; Burke, K.; Ernzerhof, M. *Phys. Rev. Lett.* **1996**, *77*, 3865.
- (26) Shi, X. Q.; Zhang, R. Q.; Minot, C.; Hermann, K.; Van Hove, M. A.; Wang, W. H.; Lin, N. *J. Phys. Chem. Lett.* **2010**, *1*, 2974.
- (27) Wang, W. H.; Shi, X. Q.; Lin, C. S.; Zhang, R. Q.; Minot, C.; Van Hove, M. A.; Hong, Y. N.; Tang, B. Z.; Lin, N. *Phys. Rev. Lett.* **2010**, *105*, 126801.
- (28) Tersoff, J.; Hamann, D. R. *Phys. Rev. B* **1985**, *31*, 805.